High Efficiency Multi-Functional All-Optical Logic Gates Based on MIM Plasmonic Waveguide Structure with the Kerr-Type Nonlinear Nano-Ring Resonators

Yaw-Dong Wu[*]

Abstract—In this paper, high efficiency multi-functional all-optical logic gates based on a metal-insulator-metal (MIM) plasmonic waveguide structure with Kerr-type nonlinear nano-ring resonators are proposed. The proposed structure consists of three straight input ports, eight nano-ring resonators filled with the Kerr-type nonlinear medium, and one straight output port. By fixing the input signal power and properly changing the control power, it can be used to design high efficiency multi-functional all-optical logic gates. The numerical results show that the proposed Kerr-type nonlinear plasmonic waveguide structures could really function as all-optical XOR/NXOR, AND/NAND, and OR/NOR logic gates in the optical communication spectral region. The transmission efficiency of the high logic state is higher than 95%, and that of the low logic state is about 0% at the wavelength 1310 nm. The performance of the proposed logic gates was analyzed and simulated by the finite element method (FEM).

1. INTRODUCTION

Recently, surface plasmon waveguide structures are popularly used to design all-optical devices. One of the most important surface plasmon polaritons (SPPs) characteristics is that electromagnetic wave can couple with propagating free electron oscillation at metal-dielectric interfaces. SPPs have promising application on ultra-compact integrated optical circuits because they can overcome the conventional diffraction limit and can manipulate light on sub-wavelength scales [1–3]. Metal-insulator-metal (MIM) optical waveguide structures can strongly confine the optical beam in the insulator region. Many plasmonic components based on the MIM waveguides have been demonstrated by numerical simulations and/or experiments [4–15]. In the past few years, there has been great interest in the possibility of using nonlinear optical waveguide devices as ultrafast photonic devices for optical signal processing and optical communication systems. All-optical switching devices and logic gates based on the optical Kerr effect in a nonlinear waveguide have been of particular interest for high-bit rate optical communication and optical computing systems. The conventional all-optical Kerr-type nonlinear waveguide structures containing one or more medium, whose refractive index depends on the local intensity, have stimulated a great deal of theoretical and experimental study. Several conventional all-optical devices using optical nonlinearity have been proposed and implemented [16–29]. However, most of the conventional all-optical devices suffer from limitations such as big size (in ∼ mm order), simultaneous output, and being difficult to perform chip scale integration. Recently, there has been great interest in the possibility of using nonlinear MIM plasmonic optical waveguide devices as ultrafast photonic devices for optical signal processing and optical communication systems. All-optical plasmonic switches and logic gates

based on Kerr-type nonlinear optical effect have been of particular interest for high-bit rate optical communication and optical computing systems.

Recently, some authors have proposed all-optical logic gates based on MIM plasmonic waveguide resonators. Bian and Gong [30] proposed compact all-optical interferometric logic gates based on one-dimensional MIM plasmonic waveguide structures. They used multi-channel MIM plasmonic waveguide configurations to design the whole set of fundamental all-optical logic gates. Chen et al. [31] proposed a novel design of ultrasmall multifunctional Boolean logic gates based on a couple metal gap waveguide structure. Dolatabady and Granpayeh [32] proposed all-optical logic gates based on two dimensional plasmonic waveguides with nano-ring resonators. Wang et al. [33] proposed all-optical quasi logic gates, demonstrated by means of polarization-dependent four-wave mixing, based on MIM plasmonic waveguide structures filled with a Kerr-type nonlinear medium. Nozhat and Granpayeh [34] proposed a nonlinear plasmonic T-shaped switch and three optical logic gates based on square-shaped ring resonators. Wen et al. [35] proposed broadband plasmonic logic input sources constructed with dual square ring resonators and dual waveguides. The proposed plasmonic waveguide structure can be used as the broadband illuminating sources for three input logic gates, such as the AND gate or OR gate. Yc et al. [36] designed a compact logic device based on plasmonic-induced transparency. The proposed plasmonic waveguide structure could implement the function of logical operations XOR and XNOR simultaneously. Abdulnabi and Abbas [37, 38] proposed all-optical logic gates based on nanoring insulator-metal-insulator plasmonic waveguides at optical communications band and all-optical combinational logic circuits based on nano-ring insulator-metal-insulator plasmonic waveguides. Shekhar et al. [39] proposed all optical OR/NOR logic gate using micro-ring resonator based switching activity. Abbas and Abdulnabi [40] proposed plasmonic reversible logic gates. Noor et al. [41] proposed the modeling and optimization of plasmonic detectors for beyond-CMOS plasmonic majority logic gates. Fakhruldeen and Mansour [42] proposed the design and simulation of plasmonic NOT gate based on insulator-metal-insulator (IMI) waveguides. However, in the previous works, the normalized transmission efficiencies of the high logic states of the proposed plasmonic all-optical logic gates in the previous works are not high enough, about 20%–80%. Most of the plasmonic waveguide structures proposed in the previous works are linear cases. In general, nonlinear optical effects are more suitable for designing all-optical switches or logic gates than the linear ones in the applications of high-bit rate optical signal processing and optical communication systems. In order to improve the normalized transmission efficiency of the high logic states, the Kerr-type nonlinear optical effect was used to design all-optical plasmonic logic gates. In this manuscript, high efficiency multi-functional all-optical logic gates based on MIM plasmonic waveguide structures with Kerr-type nonlinear nano-ring resonators are proposed. The numerical results show that the proposed Kerr-type nonlinear plasmonic waveguide structures could really function as all-optical XOR/NXOR, AND/NAND, and OR/NOR logic gates in the optical communication spectral region. The normalized transmission efficiency of the high logic state for each logic gate is higher than 95%, and that of the low logic state is about 0%. The proposed all-optical logic gates based on MIM plasmonic waveguide structures with Kerr-type nonlinear nano-ring resonators can be implemented by a lithography technique or the standard Complementary Metal-Oxide-Semiconductor (CMOS) fabrication technology [43–45]. To the best of my knowledge, this is the first time to use the MIM plasmonic waveguide structure with the Kerr-type nonlinear nano-ring resonators to design high efficiency multi-functional all-optical logic gates. The performance of logic gates was analyzed and simulated by the FEM. The proposed all-optical logic gates have great advantages of small size and low pumping light intensity. It would be a potential key component in the applications of ultra-compact all-optical integrated photonic circuits.

2. ANALYSIS

In general, the interface between semi-infinite materials having positive and negative dielectric constants can effectively guide transverse magnetic (TM) surface waves. Because the width of the MIM plasmonic waveguide is much smaller than the wavelength, only the fundamental TM waveguide mode can propagate. The dispersion equation for TM mode in the waveguide is given by [46]:

$$\varepsilon_d k_m + \varepsilon_m k_d \tanh\left(\frac{k_d}{2}w\right) = 0 \tag{1}$$

where the parameters k_d and k_m are defined as $k_d = (\beta^2 - \varepsilon_d k_0^2)^{\frac{1}{2}}$ and $k_m = (\beta^2 - \varepsilon_m k_0^2)^{\frac{1}{2}}$. ε_d and ε_m are the dielectric constants of the insulator and the metal, respectively. $k_0 = 2\pi/\lambda$ is the free-space wave vector. The propagation constant β is represented as effective index $n_{eff} = \beta/k_0$ of the waveguide for SPPs. In the paper, the dielectric is assumed to be air with $\varepsilon_d = 1$ and the metal to be silver whose imaginary part of relative permittivity is smaller than most metals, so it has lower energy-loss and low power-absorption compared to other metals. The dielectric constant ε_m of silver can be calculated by Drude model [47]

$$\varepsilon_m(\omega) = \varepsilon_\infty - \frac{\omega_p^2}{\omega(\omega + i\gamma)} \tag{2}$$

where ε_∞ stands for the dielectric constant at infinite angular frequency with the value of 3.7, and $\omega_p = 1.38 \times 10^{16}$ Hz is the bulk plasma frequency, which represents the natural frequency of the oscillations of free conduction electrons. In addition, $\gamma = 2.73 \times 10^{13}$ Hz is the damping frequency of the oscillations, and ω is the angular frequency of the incident electromagnetic radiation. The SPPs are excited with inputting a TM-polarized plane wave. The transmission of the structure is defined as $T = P_{tr}/P_{in}$ [48]. P_{in} represents the total incident power, and P_{tr} is the transmission power. The proposed structure of single aperture-side-coupled dielectric nano-ring resonator is shown in Fig. 1, which consists of a waveguide coupled to a aperture-side-coupled dielectric nano-ring cavity filled with a Kerr-type nonlinear material. The refractive index of the Kerr-type nonlinear material can be expressed as [49]:

$$n = n_0 + n_2 I \tag{3}$$

where the value of linear refractive index n_0 is set as 1.47. The Kerr-type nonlinear medium is assumed to be Au-SiO$_2$; its nonlinear refractive index is $n_2 = 2.07 \times 10^{-9}$ cm^2/W [50]; and I is the pumping beam intensity. The dielectric constant of the Kerr-type nonlinear medium in the nano-ring resonator can be changed by varying the intensity of the pumping light.
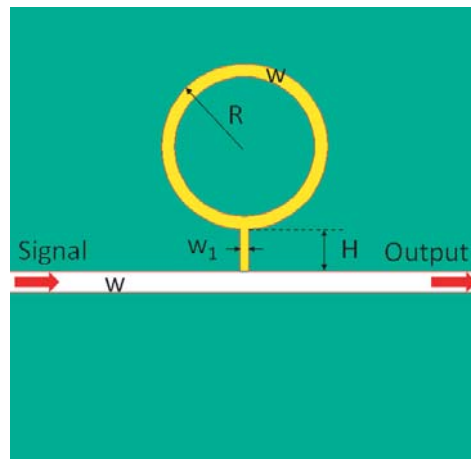

Figure 1. The nonlinear aperture-side-coupled dielectric single nano-ring resonator filled with the Kerr-type nonlinear medium.

3. NUMERICAL RESULTS AND DISCUSSIONS

Figure 1 shows the proposed MIM plasmonic waveguide structure with single nonlinear aperture-side-coupled dielectric nano-ring resonator. The parameters of the proposed structure are set to $w = 50$ nm, $w_1 = 20$ nm, $H = 100$ nm, and $R = 280$ nm. The influence of the radius of the nano-ring resonator at the resonant wavelengths is analyzed by the FEM, with the perfectly matched layer (PML) absorbing boundary conditions at all boundaries of the simulation domain. The grid sizes are chosen to be $\Delta x = \Delta y = 5$ nm and $\Delta t = \Delta x/2c$. The radius is set as variable while the other parameters are

fixed as above. Fig. 2(a) shows the transmission spectra of the single ring resonator structure with radii varying from $R = 270$ nm to 290 nm. The numerical results show that the resonant peak-wavelengths have a red-shift with increase of the radii of the nano-ring resonator. Fig. 2(b) shows that the relationship between the resonant peak-wavelengths and the radii of the nano-ring resonator is approximately linear. Fig. 3 shows the relationship between the resonant peak-wavelengths and the width of the coupling rectangular aperture w_1. The resonant peak-wavelengths have a red-shift with decrease of the width of the coupling rectangular aperture. Fig. 4 shows the normalized transmission spectra for fixed $R = 290$ nm, $w_1 = 20$ nm, $w = 50$ nm with the height of the coupling rectangular aperture varying from $H = 60$ nm to 140 nm. The resonant peak-wavelengths have a red-shift with increasing the height of the coupling rectangular aperture H. By properly changing the radii of the nano-ring resonators, and the width and height of the coupling rectangle waveguide, the operating wavelength can be tuned easily. For the resonance of a ring resonator to take place, the circumference

(a)   (b)
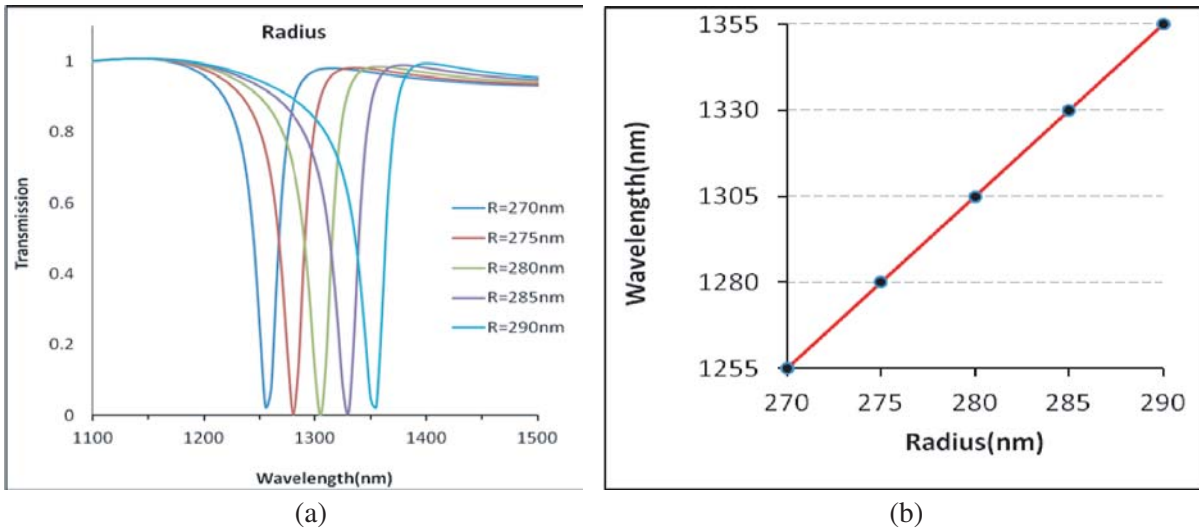
Figure 2. (a) Transmission spectra of the single ring resonator structure with different radius for $R = 270$ nm $\sim$ 290 nm, (b) the relationship between the resonant wavelengths and the radii of the nano-ring resonator.
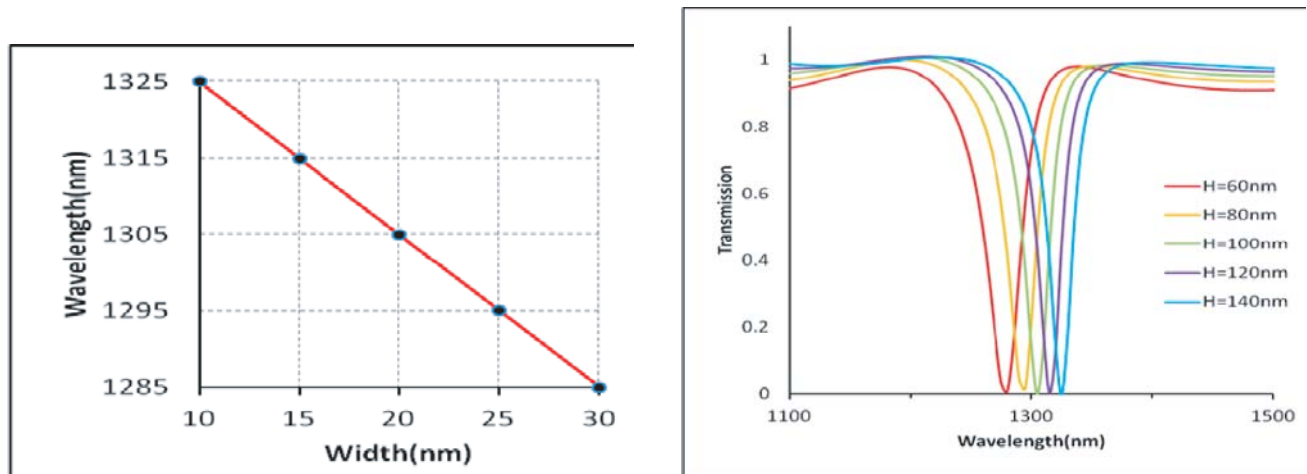
Figure 3. The relationship between the resonant peak-wavelengths and the width of the coupling rectangular aperture w_1.

Figure 4. Transmission spectra of the single ring resonator structure with different height of the coupling rectangular aperture $H = 60$ nm $\sim$ 140 nm.

of the ring must be an integer multiple of the wavelength of the light. And the mode number must be a positive integer for resonance to take place. When the incident light contains multiple wavelengths, only the resonant wavelengths can propagate through the ring resonator fully. Hence, a ring resonator will have several resonant modes. The two photon absorption and induced free carrier effect in the Kerr-type nonlinear medium are not considered in this numerical simulation process. When the TM waves are launched into the proposed MIM plasmonic waveguide structure to excite the SPPs, the incident waves will be coupled into the MIM plasmonic waveguide structure, and the SPPs are formed on the interfaces between the insulator and metal. Meanwhile, the incident waves will be coupled to the nano-ring resonators through the coupling rectangle waveguide. The standing wave modes in the nano-ring resonators will be excited if the resonant condition is satisfied. The resonant modes will be very sensitive to the dielectric constant which can be changed by the input signal and pump light due to the Kerr-type nonlinear effect of the nonlinear medium. In the following, the high efficiency multi-functional all-optical logic gates based on the MIM plasmonic waveguide structure with Kerr-type nonlinear nano-ring resonators are proposed, as shown in Fig. 5. The proposed structure consists of three straight input ports, eight nano-ring resonators filled with the Kerr-type medium, and one straight output port. It can be used to design six all-optical logic gates, such as XOR/NXOR, AND/NAND, and OR/NOR logic gates. The dielectric constant of the Kerr-type nonlinear medium in the nano-ring resonator can be changed by varying the intensity of the pumping light. The transmission spectra will have a red shift with increasing the intensity of the pumping light. The gate functions of the proposed MIM plasmonic waveguide structure can be realized by the principle of constructive and destructive interferences between the input signal and control signals. By properly changing the intensity of the pumping light and optimizing the parameters of the proposed MIM plasmonic waveguide structure with the Kerr-type nonlinear nano-ring resonators, it can be really used to design multi-functional all-optical logic gates. The gate functions of the proposed MIM plasmonic waveguide structure can be realized by the principle of constructive and destructive interferences between the input signal and control signals.
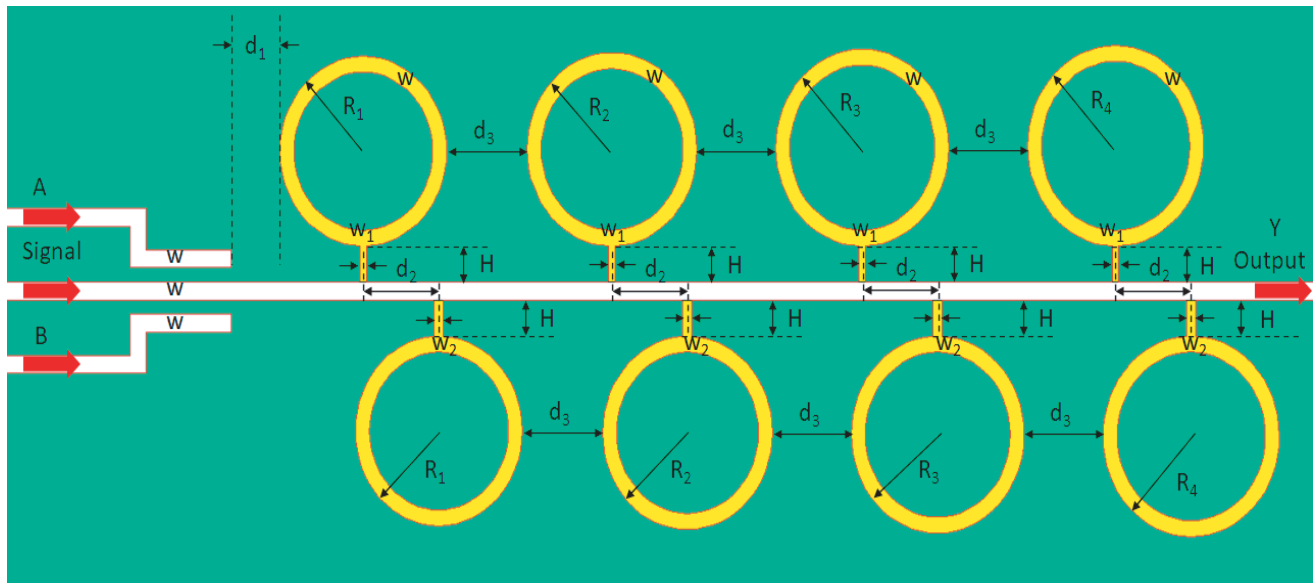
Figure 5. The proposed high efficiency multi-functional all-optical logic gate based on the MIM plasmonic waveguide structure with Kerr-type nonlinear nano-ring resonators.

3.1. AND Gate

The proposed MIM plasmonic waveguide structure with eight nano-ring resonators filled with the Kerr-type nonlinear medium was used to design an all-optical AND logic gate, as shown in Fig. 5. The optimal parameters of the proposed structure are chosen: $R_1 = 275$ nm, $R_2 = 279$ nm, $R_3 = 282$ nm,

(a)

(b)

(c)

(d)
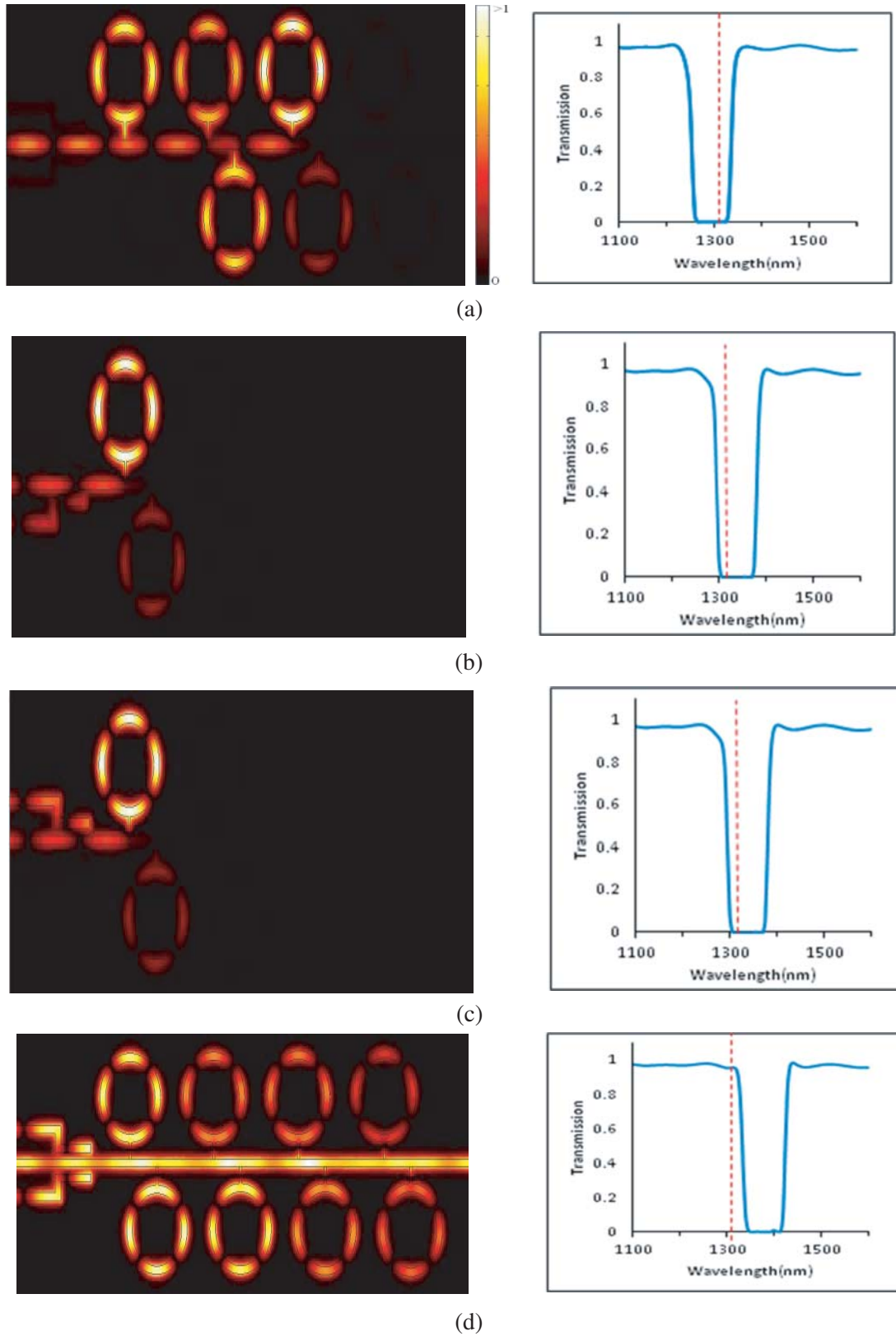
Figure 6. The normalized magnetic field distributions and the normalized transmissions of the proposed AND logic gate, when (a) $A = 0$, $B = 0$, (b) $A = 0$, $B = 1$, (c) $A = 1$, $B = 0$, (d) $A = 1$, $B = 1$.

$R_4 = 286$ nm, $H = 120$ nm, $w = 50$ nm, $w_1 = 20$ nm, $w_2 = 25$ nm, $d_1 = 90$ nm, $d_2 = 250$ nm, and $d_3 = 200$ nm. The logic function of AND logic gate is that as both of the control input ports are logic 1, the output port is logic 1; otherwise, the output port is logic 0. In this structure, the signal port is always ON with the intensity $I_0 = 1 \times 10^6$ W/cm^2, and the intensity of the ON state of the output control ports is $I_1 = 5 \times 10^7$ W/cm^2. The logic states and normalized transmissions of AND logic gates at the wavelength 1310 nm are shown in Table 1. The normalized magnetic field distributions and the normalized transmissions at the wavelength 1310 nm are also shown in Figs. 6(a)–(d). As the results shown above, the proposed plasmonic waveguide structure would function as an AND logic gate.

Table 1. The logic states and the normalized transmissions of the proposed AND logic gate at the wavelength 1310 nm.

A	B	Y	Transmission (%)
0	0	0	0%
0	1	0	0%
1	0	0	0%
1	1	1	96%

3.2. OR Gate

The proposed MIM plasmonic waveguide structure with eight-ring resonators filled with the Kerr-type nonlinear medium was used to design an all-optical OR logic gate, as shown in Fig. 5. The optimal parameters of the proposed structure are chosen, $R_1 = 275$ nm, $R_2 = 279$ nm, $R_3 = 282$ nm, $R_4 = 286$ nm, $H = 120$ nm, $w = 50$ nm, $w_1 = 20$ nm, $w_2 = 25$ nm, $d_1 = 90$ nm, $d_2 = 250$ nm. The logic function of OR logic gate is that if at least one of the control input ports is logic 1, the output port is logic 1, and if both of the control input ports are logic 0, the output port is logic 0. In this structure, the signal port is always ON with the intensity $I_0 = 1 \times 10^6$ W/cm^2, and the intensity of the ON state of the output control ports is $I_1 = 1 \times 10^8$ W/cm^2. The logic states and normalized transmissions of OR logic gates at wavelength 1310 nm are shown in Table 2. The normalized magnetic field distributions and normalized transmissions at the wavelength 1310 nm are also shown in Figs. 7(a)–(d). As the results shown above, the proposed plasmonic waveguide structure would function as an OR logic gate.

Table 2. The logic states and the normalized transmissions of the proposed OR logic gate at the wavelength 1310 nm.

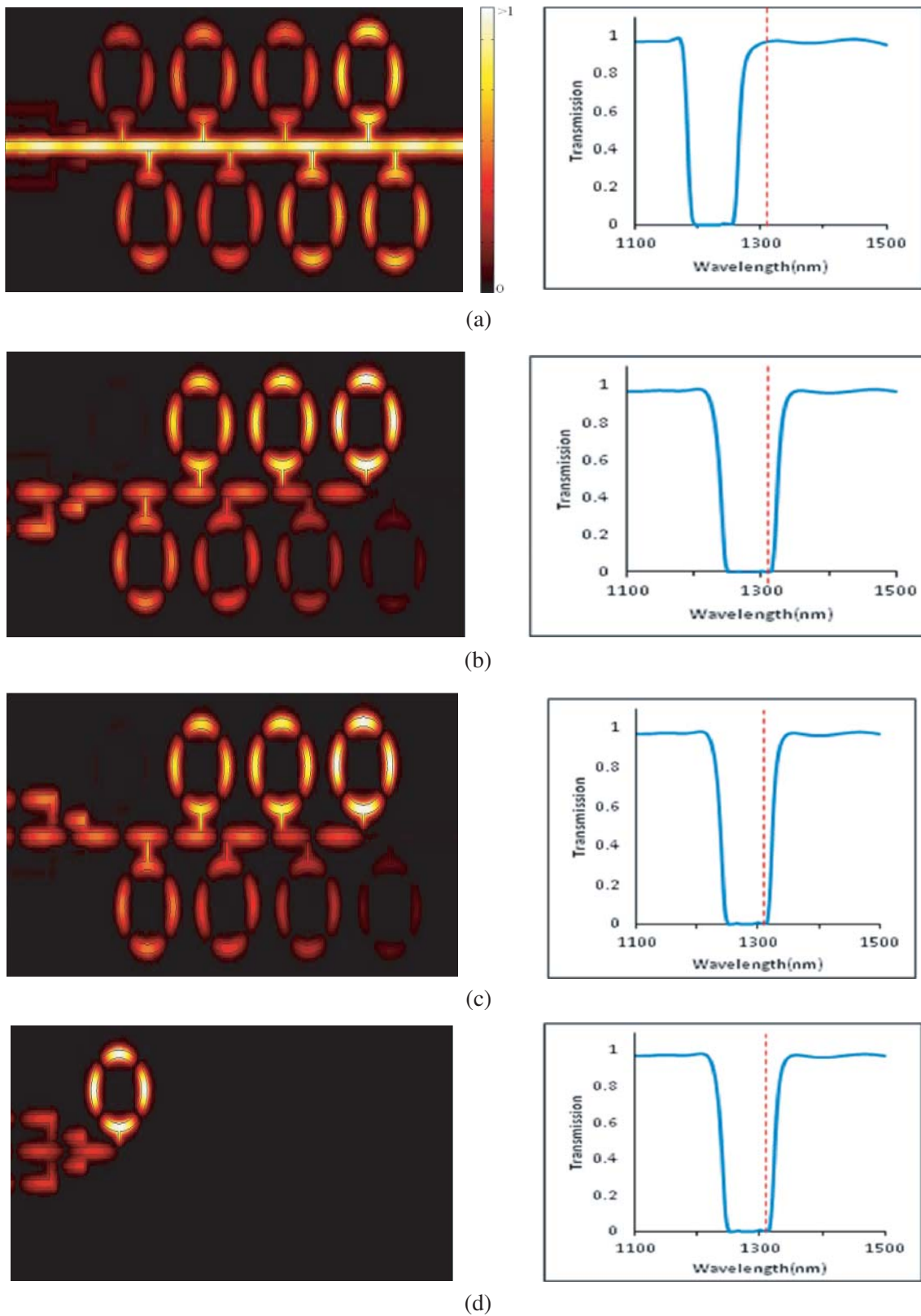| A	B	Y	Transmission (%)
0	0	0	0%
0	1	1	95%
1	0	1	95%
1	1	1	96%

3.3. NOR Gate

The proposed MIM plasmonic waveguide structure with eight nano-ring resonators filled with the Kerr-type nonlinear medium was used to design an all-optical NOR logic gate, as shown in Fig. 5. The optimal parameters of the proposed structure are chosen $R_1 = 258$ nm, $R_2 = 262$ nm, $R_3 = 265$ nm, $R_4 = 269$ nm, $H = 120$ nm, $w = 50$ nm, $w_1 = 20$ nm, $w_2 = 25$ nm, $d_1 = 90$ nm, $d_2 = 250$ nm. The logic function of NOR logic gate is that if at least one of the input control ports is logic 1, the output port is logic 0, and if both of the control input ports are logic 0, the output port is logic 1. In this structure, the signal port is always ON with the intensity $I_0 = 1 \times 10^6$ W/cm^2, and the intensity of the ON state

(a)

(b)

(c)

(d)
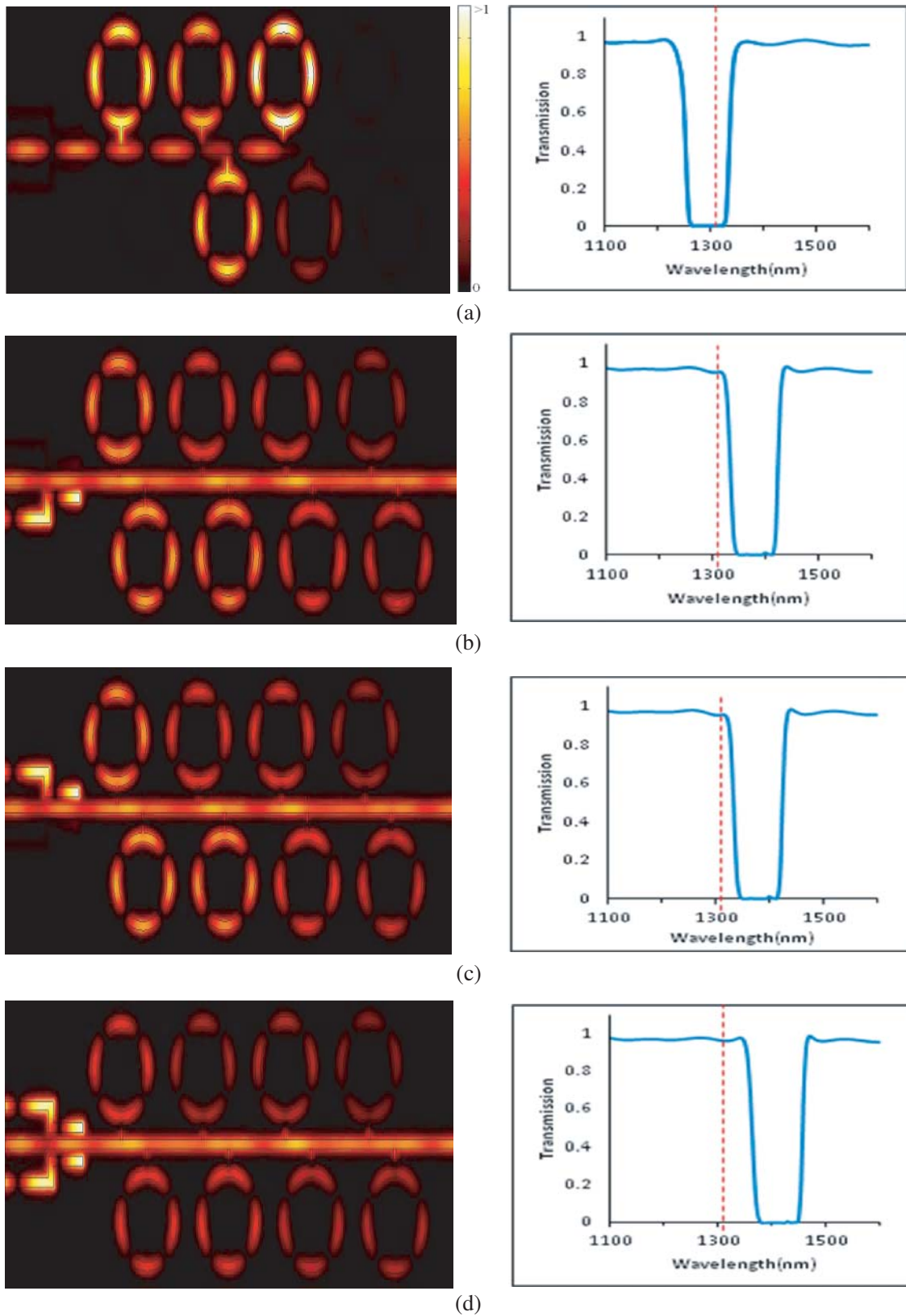
Figure 7. The normalized magnetic field distributions and the normalized transmissions of the proposed OR logic gate, when (a) $A = 0$, $B = 0$, (b) $A = 0$, $B = 1$, (c) $A = 1$, $B = 0$, (d) $A = 1$, $B = 1$.

(a)

(b)

(c)

(d)

Figure 8. The normalized magnetic field distributions and the normalized transmissions of the proposed NOR logic gate, when (a) $A = 0$, $B = 0$, (b) $A = 0$, $B = 1$, (c) $A = 1$, $B = 0$, (d) $A = 1$, $B = 1$.

of the output control ports is $I_1 = 7 \times 10^7 \, \text{W/cm}^2$. The logic states and normalized transmissions of OR logic gates are shown in Table 3. The normalized magnetic field distributions and normalized transmission are also shown in Figs. 8(a)–(d). As the results shown above, the proposed plasmonic waveguide structure would function as an NOR logic gate.

Table 3. The logic states and the normalized transmissions of the proposed NOR logic gate at the wavelength 1310 nm.

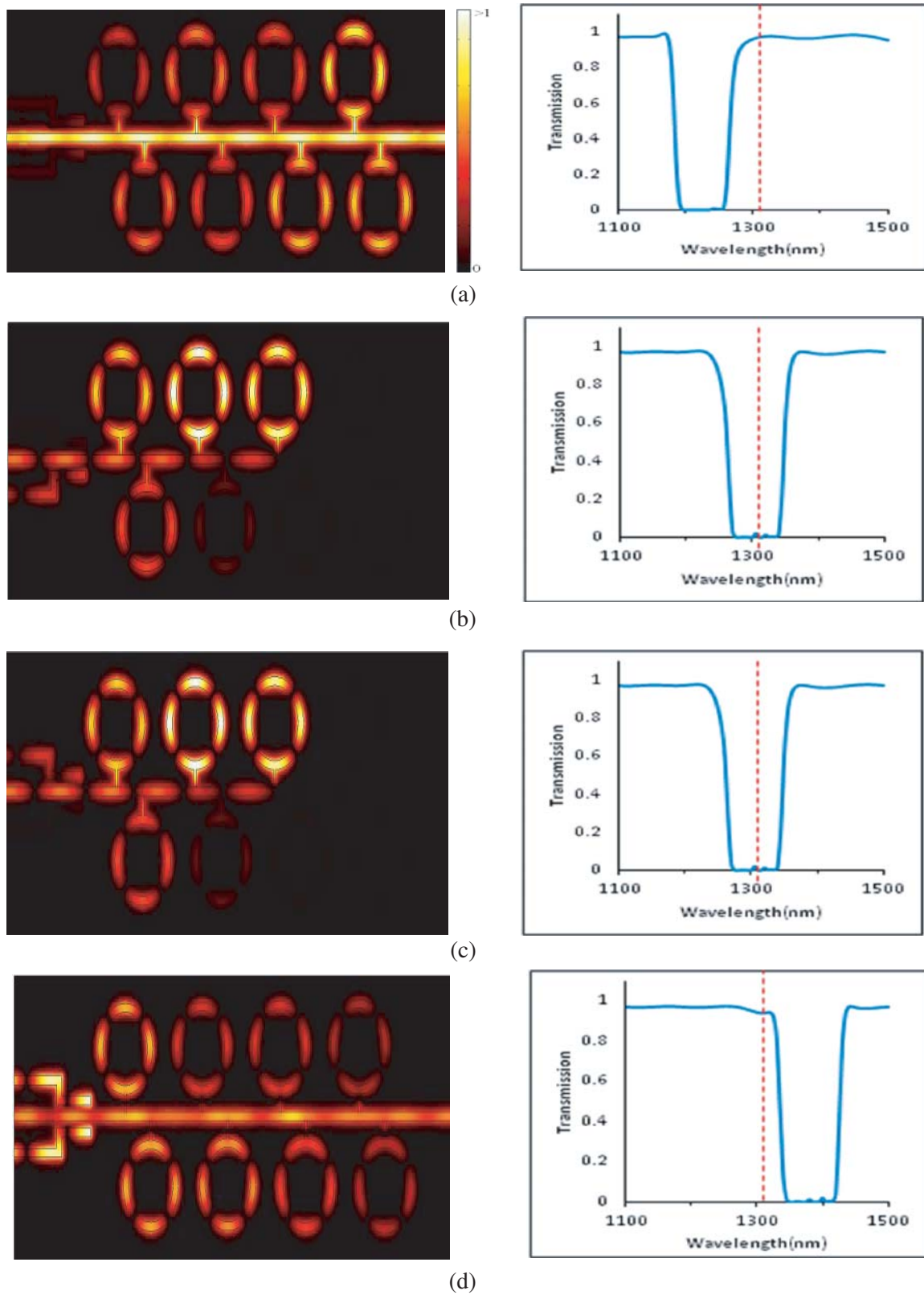| A	B	Y	Transmission (%)
0	0	1	97%
0	1	0	0%
1	0	0	0%
1	1	0	0%

3.4. XNOR Gate

The proposed MIM plasmonic waveguide structure with eight nano-ring resonators filled with the Kerr-type nonlinear medium was used to design an all-optical XNOR logic gate, as shown in Fig. 5. The optimal parameters of the proposed structure are chosen, $R_1 = 258 \, \text{nm}$, $R_2 = 262 \, \text{nm}$, $R_3 = 265 \, \text{nm}$, $R_4 = 269 \, \text{nm}$, $H = 120 \, \text{nm}$, $w = 50 \, \text{nm}$, $w_1 = 20 \, \text{nm}$, $w_2 = 25 \, \text{nm}$, $d_1 = 90 \, \text{nm}$, $d_2 = 250 \, \text{nm}$. The logic function of XNOR logic gate is that if the logic states of the control input ports are the same, the output port is logic 1; otherwise, the output port is logic 0. In this structure, the signal port is always ON with the intensity $I_0 = 1 \times 10^6 \, \text{W/cm}^2$, and the intensity of the ON state of the output control ports is $I_1 = 1.5 \times 10^8 \, \text{W/cm}^2$. The logic states and normalized transmissions of XNOR logic gates are shown in Table 4. The normalized magnetic field distributions and normalized transmissions are also shown in Figs. 9(a)–(d). As the results shown above, the proposed plasmonic waveguide structure would function as an XNOR logic gate.

Table 4. The logic states and the normalized transmissions of the proposed XNOR logic gate at the wavelength 1310 nm.
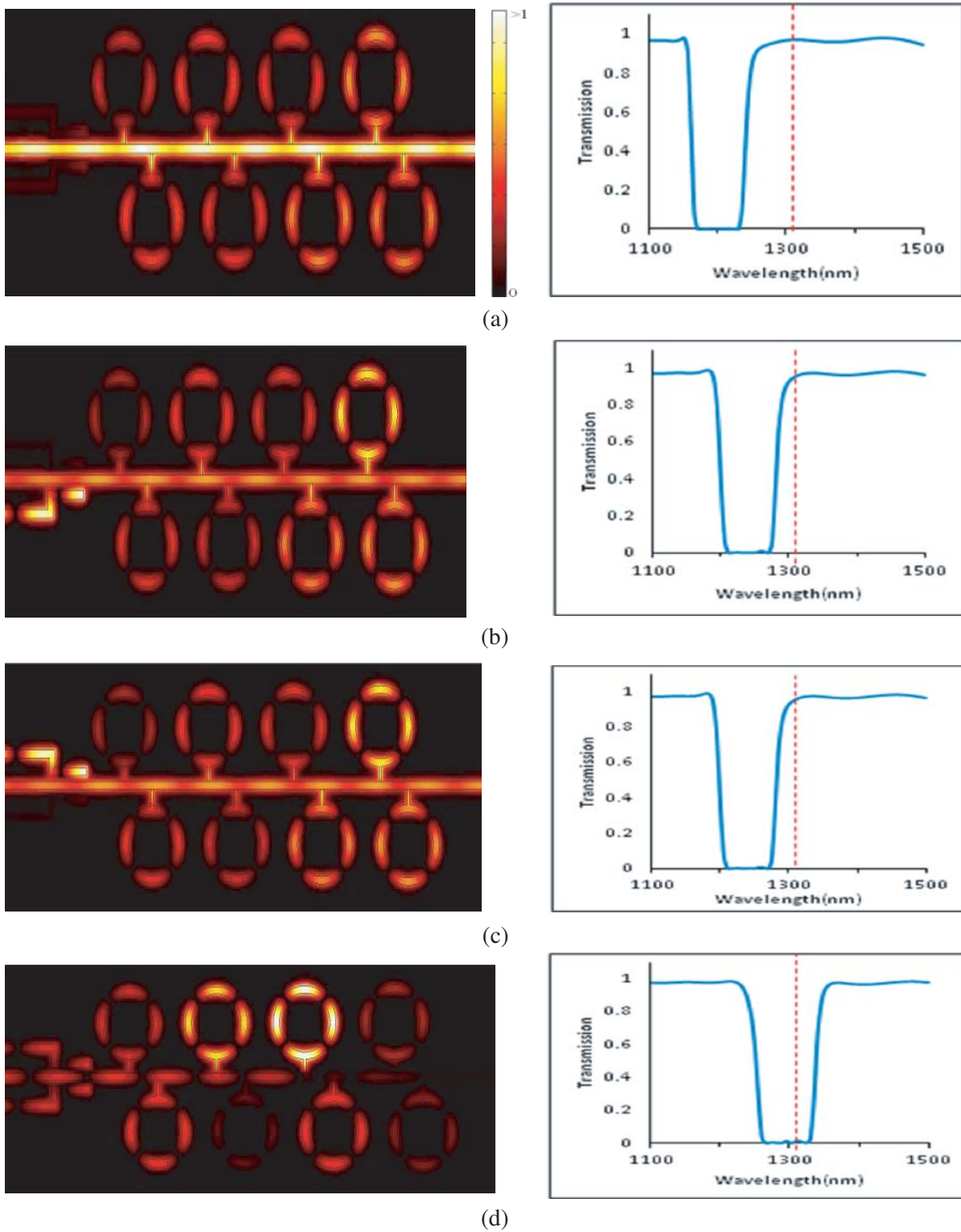
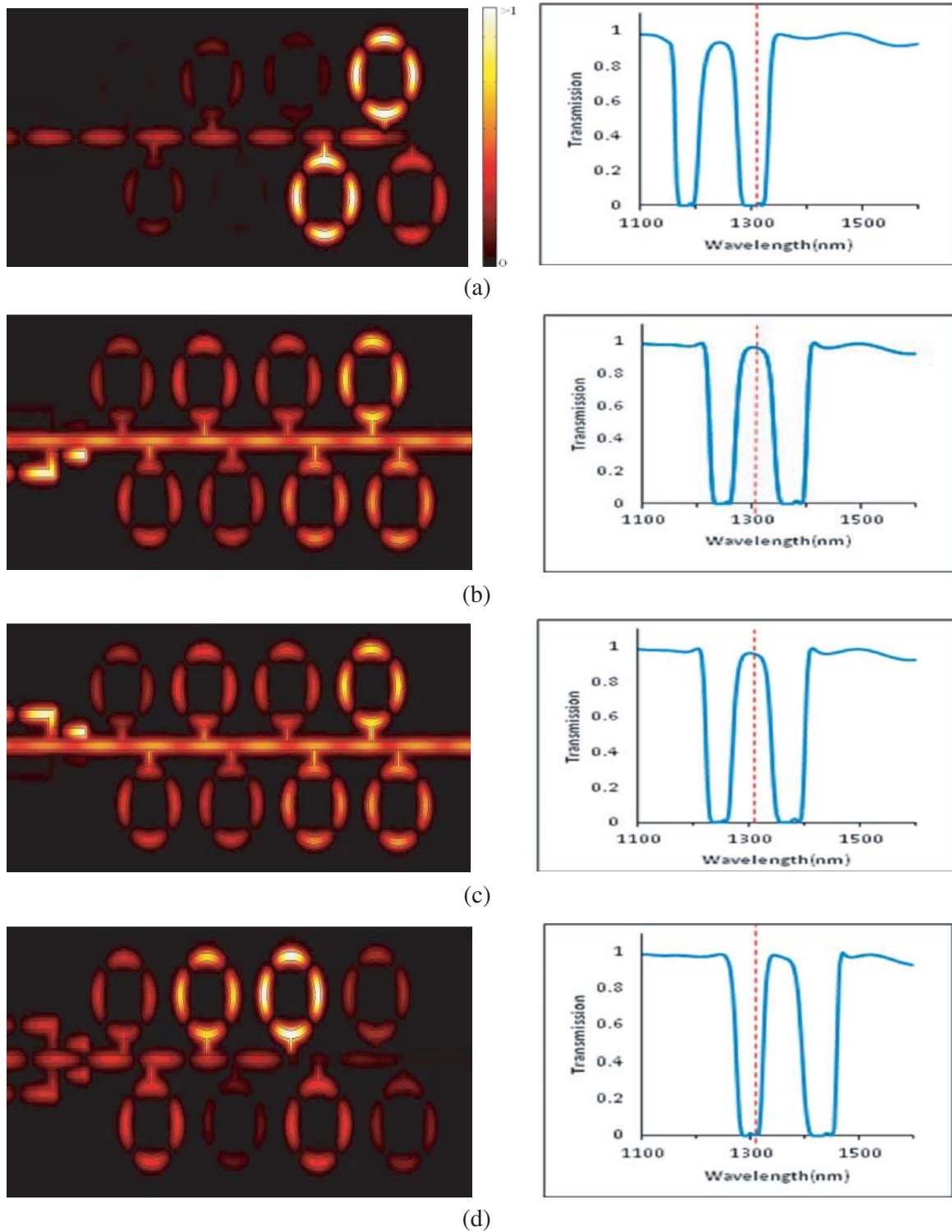| A	B	Y	Transmission (%)
0	0	1	97%
0	1	0	0%
1	0	0	0%
1	1	1	95%

3.5. NAND Gate

The proposed MIM plasmonic waveguide structure with eight nano-ring resonators filled with the Kerr-type nonlinear medium was used to design an all-optical NAND logic gate, as shown in Fig. 5. The optimal parameters of the proposed structure are chosen, $R_1 = 253 \, \text{nm}$, $R_2 = 257 \, \text{nm}$, $R_3 = 260 \, \text{nm}$, $R_4 = 264 \, \text{nm}$, $H = 120 \, \text{nm}$, $w = 50 \, \text{nm}$, $w_1 = 20 \, \text{nm}$, $w_2 = 25 \, \text{nm}$, $d_1 = 90 \, \text{nm}$, $d_2 = 250 \, \text{nm}$. The logic function of NAND logic gate is that as both of the control input ports are logic 1, the output port is logic 0; otherwise, the output port is logic 1. In this structure, the signal port is always ON with the intensity $I_0 = 1 \times 10^6 \, \text{W/cm}^2$, and the intensity of the ON state of the output control ports is $I_1 = 5 \times 10^7 \, \text{W/cm}^2$. The logic states and normalized transmissions of NAND logic gates at the wavelength 1310 nm are shown in Table 5. The normalized magnetic field distributions and normalized transmissions at the wavelength 1310 nm are also shown in Figs. 10(a)–(d). As the results shown above, the proposed plasmonic waveguide structure would function as a NAND logic gate.

Figure 9. The normalized magnetic field distributions and the normalized transmissions of the proposed XNOR logic gate, when (a) $A = 0$, $B = 0$, (b) $A = 0$, $B = 1$, (c) $A = 1$, $B = 0$, (d) $A = 1$, $B = 1$.

(a)

(b)

(c)

(d)

Figure 10. The normalized magnetic field distributions and the normalized transmissions of the proposed NAND logic gate, when (a) $A = 0$, $B = 0$, (b) $A = 0$, $B = 1$, (c) $A = 1$, $B = 0$, (d) $A = 1$, $B = 1$.

Figure 11. The normalized magnetic field distributions and the normalized transmissions of the proposed XOR logic gate, when (a) $A = 0$, $B = 0$, (b) $A = 0$, $B = 1$, (c) $A = 1$, $B = 0$, (d) $A = 1$, $B = 1$.

Table 5. The logic states and the normalized transmissions of the proposed NAND logic gate at the wavelength 1310 nm.

A	B	Y	Transmission (%)
0	0	1	97%
0	1	1	96%
1	0	1	96%
1	1	0	0%

3.6. XOR Gate

Finally, the proposed MIM plasmonic waveguide structure with eight nano-ring resonators filled with the Kerr-type nonlinear medium was used to design an all-optical XOR logic gate, as shown in Fig. 5. The optimal parameters of the proposed structure are chosen, $R_1 = 253$ nm, $R_2 = 257$ nm, $R_3 = 280$ nm, $R_4 = 283$ nm, $H = 120$ nm, $w = 50$ nm, $w_1 = 20$ nm, $w_2 = 25$ nm, $d_1 = 90$ nm, $d_2 = 250$ nm. The logic function of XOR logic gate is that if the logic states of the control input ports are the same, the output port is logic 0; otherwise, the output port is logic 1. In this structure, the signal port is always ON with the intensity $I_0 = 1 \times 10^6$ W/cm^2, and the intensity of the ON state of the output control ports is $I_1 = 6 \times 10^7$ W/cm^2. The logic states and normalized transmissions of XNOR logic gates are shown in Table 6. The normalized magnetic field distributions and normalized transmissions are also shown in Figs. 11(a)–(d). As the results shown above, the proposed plasmonic waveguide structure would function as an XOR logic gate.

Table 6. The logic states and the normalized transmissions of the proposed XOR logic gate at the wavelength 1310 nm.

A	B	Y	Transmission (%)
0	0	0	0%
0	1	1	96%
1	0	1	96%
1	1	0	0%

4. CONCLUSIONS

In this paper, high efficiency multi-functional all-optical logic gates based on the MIM plasmonic waveguide structures with the Kerr-type nonlinear nano-ring resonators have been proposed. The dielectric constant of the Kerr-type nonlinear medium in the nano-ring resonators can be changed by varying the intensity of the pumping light. By fixing the input signal power and properly changing the control power, we can design multi-functional all-optical logic gates. In order to improve the normalized transmission efficiency of the high logic states, the Kerr-type nonlinear optical effect was used to design the all-optical plasmonic logic gates. The numerical results show that the proposed Kerr-type nonlinear plasmonic waveguide structures could really function as all-optical XOR/NXOR, AND/NAND, and OR/NOR logic gates in the optical communication spectral region. The normalized transmission efficiency of the high logic state for each logic gate is higher than 95%, and that of the low logic state is about 0%. To the best of my knowledge, it is the first time to use the MIM plasmonic waveguide structure with the Kerr-type nonlinear nano-ring resonators to design high efficiency multi-functional all-optical logic gates. Since the resonant peak-wavelengths have a red-shift with increase of the radii of the nano-ring resonators, by properly increasing the radii of the nano-ring resonators the operating wavelength can also be shifted to 1550 nm. The performance of logic gates was analyzed and simulated by the FEM. The proposed all-optical logic gates have great advantages of small size and low pumping light intensity. They would be potential key components in the applications of ultra compact all-optical integrated photonic circuits.

REFERENCES

1. Raether, H., *Surface Plasmons on Smooth and Rough Surfaces and on Gratings*, Springer-Verlag, Berlin, Germany, 1988.

2. Barnes, W. L., A. Dereux, and T. Ebbesen, "Surface plasmon subwavelength optics," *Nature*, Vol. 424, 824–830, 2003.

3. Takahara, J., Y. Suguru, T. Hiroaki, A. Morimoto, and T. Kobayashi, "Guiding of a one-dimensional optical beam with nanometer diameter," *Opt. Lett.*, Vol. 22, 475–477, 1997.

4. Veronis, G., Z. Yu, S. E. Kocabas, D. A. B. Miller, M. L. Brongersma, and S. Fan, "Metal-dielectric-metal plasmonic waveguide devices for manipulating light at the nanoscale," *Chin. Opt. Lett.*, Vol. 7, 302–308, 2009.

5. Han, Z., E. Forsberg, and S. He, "Surface plasmon Bragg gratings formed in metal-insulator-metal waveguides," *IEEE Photon. Technol.*, Vol. 19, 91–93, 2007.

6. Park, J., H. Kim, and B. Lee, "High order plasmonic Bragg reflection in the metal-insulator-metal waveguide Bragg grating," *Opt. Express*, Vol. 16, 413–425, 2008.

7. Hosseini, A., H. Nejati, and Y. Massoud, "Modeling and design methodology for metal-insulator-metal plasmonic Bragg reflectors," *Opt. Express*, Vol. 16, 1475–1480, 2008.

8. Hosseini, A. and Y. Massoud, "A low-loss metal-insulator-metal plasmonic Bragg reflector," *Opt. Express*, Vol. 14, 11318–11323, 2006.

9. Pu, M., N. Yao, C. Hu, X. Xin, Z. Zhao, C. Wang, and X. Luo, "Directional coupler and nonlinear Mach-Zehnder interferometer based on metal insulator-metal plasmonic waveguide," *Opt. Express*, Vol. 18, 21030–21037, 2010.

10. Hosseini, A. and Y. Massoud, "A rectangular metal-insulator-metal based nanoscale plasmonic resonator," *IEEE-NANO*, 81–84, 2007.

11. Anglin, K., D. C. Adams, T. Ribaudo, and D. Wasserman, "Toothed mid-infrared metal-insulator-metal waveguides," *CLEO*, CTuS4, 2011.

12. Bian, Y. and Q. Gong, "Compact all-optical interferometric logic gates based on one-dimensional metal-insulator-metal structures," *Opt. Comm.*, Vol. 313, 27–35, 2014.

13. Chen, Z. Q., J. Chen, Y. D. Li, D. Pan, W. Q. Lu, Z. Q. Hao, J. J. Xu, and Q. Sun, "Simulation of nanoscale multifunctional interferometric logic gates based on coupled metal gap waveguides," *IEEE Photonics Technology Letters*, Vol. 24, 1366–1368, 2012.

14. Dolatabady, A. and N. Granpayeh, "All optical logic gates based on two dimensional plasmonic waveguides with nanodisk resonators," *J. O. S. K.*, Vol. 16, 432, 2012.

15. Wu, Y. D., "High transmission efficiency wavelength division multiplexer based on metal-insulator-metal plasmonic waveguides," *OSA/IEEE J. of Lightwave Techn.*, Vol. 32, 4242, 2014.

16. Pramono, Y. H. and Endarko, "Nonlinear waveguides for optical logic and computation," *J. Nonlinear Opt. Phys. Mater.*, Vol. 10, 209–222, 2001.

17. Wu, Y. D., "New all-optical switch based on the spatial soliton repulsion," *Opt. Express*, Vol. 14, 4005, 2006.

18. Wu, Y. D., M. L. Whang, M. H. Chen, and R. Z. Tasy, "All-optical switch based on the local nonlinear Mach-Zehnder interferometer," *Opt. Express*, Vol. 15, 9883, 2007.

19. Radwell, N., C. McIntyre, A. J. Scroggie, G. L. Oppo, W. J. Firth, and T. Ackemann, "Switching spatial dissipative solitons in a VCSEL with frequency selective feedback," *Eur. Phys. J. D*, Vol. 59, 121, 2010.

20. Sarma, K., "Vector soliton switching in a fiber nonlinear directional coupler," *Opt. Comm.*, Vol. 284, 186, 2011.

21. Hatami, M., R. Attarzadeh, and A. Gharaati, "Design of an ultra-fast all-optical dark soliton switch in a Three-core Nonlinear Directional Coupler (TNLDC) made of chalcogenide glasses," *J. Nonlinear Optic. Phys. Mat.*, Vol. 21, 1250038, 2012.

22. Karimi, S., M. Ebnali-Heidari, and F. Forootan, "Design and modelling of a $1 \times n$ all-optical nonlinear Mach-Zehnder switch controlled by wavelength and input power," *Progress In Electromagnetics Research M*, Vol. 28, 101–113, 2013.

23. Liu, W.-J. and M. Lei, "All-optical switches using solitons within nonlinear fibers," *Journal of Electromagnetic Waves and Applications* Vol. 27, No. 18, 2288–2297, 2013.

24. Zhong, H., B. Tian, Y. Jiang, M. Li, P. Wang, and W.-J. Liu, "All-optical soliton switching for the asymmetric fiber couplers," *Eur. Phys. J. D*, Vol. 67, 1, 2013.

25. Wu, Y. D., "All-optical logic gates by using multibranch waveguide structure with localized optical nonlinearity," *IEEE J. Sel. Top. Quantum. Electron.*, Vol. 11, 307, 2005.

26. Serak, S. V., N. V. Tabiryan, M. Peccianti, and G. Assanto, "Spatial soliton all-optical logic gates," *IEEE Photon. Techn. Lett.*, Vol. 18, 1287, 2006.

27. Wu, Y. D., T. T. Shih, and M. H. Chen, "New all-optical logic gates based on the local nonlinear Mach-Zehnder interferometer," *Opt. Express*, Vol. 16, 248, 2008.

28. Corbelli, M. M., F. Garzia, and R. Cusani, "All-optical EXOR for cryptographic application based on spatial solitons," *J. of Info. Security*, Vol. 4, 180, 2013.

29. Kubota, Y. and T. Odagaki, "Logic gates based on soliton transmission in the toda lattice," *Adv. in Appl. Phys.*, Vol. 1, 29, 2013.

30. Bian, Y. and Q. Gong, "Compact all-optical interferometric logic gates based on one-dimensional metal-insulator-metal structures," *Opt. Comm.*, Vol. 313, 27, 2014.

31. Chen, Z., J. Chen, Y. Li, D. Pen, W. Lu, Z. Hao, J. Xu, and Q. Sun, "Simulation of nanoscale multifuntional interferometric logic gates based on coupled metal gap waveguides," *IEEE Photon. Technol. Lett.*, Vol. 24, 1366, 2012.

32. Dolatabady, A. and N. Granpayeh, "All optical logic gate based on two dimensional plasmonic waveguides with nanodisk resonators," *J. of the Opt. Soci. of Korea*, Vol. 16, 432, 2012.

33. Wang, L., L. Yan, Y. Guo, K. Wen, W. Pan, and B. Luo, "Optical quasi logic based on polarization-dependent four-wave mixing in subwavelength metallic waveguides," *Opt. Express*, Vol. 21, 14442, 2013.

34. Nozhat, N. and N. Granpayeh, "All-optical logic gates based on nonlinear plasmonic ring resonators," *Appl. Opt.*, Vol. 54, 7944, 2015.

35. Wen, J., J. Chen, K. Wang, B. Dai, Y. Hung, and D. Zhang, "Broadband plasmonic logic input sources constructed with dual square ring resonators and dual waveguides," *IEEE Photon. J.*, Vol. 8, 4801209, 2016.

36. Yc, Y., Y. Xic, Y. Liu, S. Wang, J. Zhang, and Y. Liu, "Design of a compact logic device based on plasmonic-induced transparency," *IEEE Photon. J.*, Vol. 29, 647, 2016.

37. Abdulnabi, S. H. and M. N. Abbas, "All-optical logic gates based on nanoring insulator-metal-insulator plasmonic waveguides at optical communications band," *Journal of Nanophotonics*, Vol. 13, No. 1, 16009, 2019.

38. Abdulnabi, S. H. and M. N. Abbas, "Design an all-optical combinational logic circuits based on nano-ring insulator-metal-insulator plasmonic waveguides," *Photonics*, Vol. 6, No. 1, 30, 2019.

39. Shekhar, P., A. Kumar, A. Ahmad, and M. Srivastava, "All optical OR/NOR logic gate using the micro-ring resonator based switching activity," *International Conference on Electrical, Electronics and Computer Engineering (UPCON)*, 2019.

40. Abbas, M. N. and S. H. Abdulnabi, "Plasmonic reversible logic gates," *Journal of Nanophotonics*, Vol. 14, No. 01, 1, 2019.

41. Noor, S. L., K. Dens, P. Reynaert, F. Catthoor, D. Lin, P. V. Dorpe, and A. Naeemi, "Modeling and optimization of plasmonic detectors for beyond-CMOS plasmonic majority logic gates," *OSA/IEEE J. of Lightwave Technol.*, Vol. 38, 5092, 2020.

42. Fakhruldeen, H. F. and T. S. Mansour, "Design and simulation of plasmonic NOT gate based on insulator-metal-insulator (IMI) waveguides," *Advanced Electromagnetics*, Vol. 9, 91, 2020.

43. Sederberg, S., V. Van, and A. Y. Elezzabi, "Monolithic integration of plasmonic waveguides into a complimentary metal-oxide-semiconductor- and photonic-compatible platform," *Appl. Phys. Lett.*, Vol. 96, 121101, 2010.

44. Choo, H., M. K. Kim, M. Staffaroni, T. J. Seok, J. Bokor, S. Cabrini, P. J. Schuck, M. C. Wu, and E. Yablonovitch, "Nanofocusing in a metal-insulator-metal gap plasmon waveguide with a three-dimensional linear taper," *Nat. Photonics*, Vol. 6, 838–844, 2012.

45. Kwon, M. S., J. S. Shin, S. Y. Shin, and W. G. Lee, "Characterizations of realized metal-insulator-silicon-insulator-metal waveguides and nanochannel fabrication via insulator removal," *Opt. Express*, Vol. 20, 21875–21887, 2012.

46. Sullivan, D., D. Borup, and O. Gandhi, "Use of the finite-difference time-domain method in calculating EM absorption in human tissues," *IEEE Trans. Biomed. Eng.*, Vol. 34, 148, 1987.

47. Adhidjaja, J. and G. Horhmann, "A finite-difference algorithm for the transient electromagnetic response of a three-dimensional body," *Geophysics J. Int.*, Vol. 98, 233, 1989.

48. Piket-May, M. and A. Taflove, "Electrodynamics of visible-light interactions with the vertebrate retinal rod," *Opt. Lett.*, Vol. 18, 568, 1993.

49. Caorsi, S., A. Massa, and M. Pastorino, "Computation of electromagnetic scattering by nonlinear bounded dielectric objects: A FDTD approach," *Microwave Opt. Technol. Lett.*, Vol. 7, 788, 1994.

50. Tao, J., Q. J. Wang, and X. G. Huang, "All-optical plasmonic switches based on coupled nano-disk cavity structures containing nonlinear material," *Plasmonics*, Vol. 6, 753, 2011.